Extensive Experimental and Analytical Investigation of the Aerodynamic Flow Field of Labyrinth Seals with Innovative Liner Configurations

Extensive Experimental and Analytical Investigation of the Aerodynamic Flow Field of Labyrinth Seals with Innovative Liner Configurations

Lisa Hühn, Julius Wilhelm, Corina Schwitzke, Hans-Jörg Bauer
Institute of Thermal Turbomachinery (ITS), Karlsruhe Institute of Technology (KIT), Karlsruhe, Germany

E-mail: lisa.huehn@kit.edu

Abstract. The state-of-the-art sealing systems in aircraft engines are labyrinth seals to regulate mass flow between rotating components. To prevent structural damage of vital parts during a rubbing process, abradable liner configurations with hollow body structures are applied on the stator. Compared to smooth stator surfaces, these structures increase the cross-sectional area of the sealing gap and, thus, lead to a higher leakage. The aim of this paper is to identify the main geometrical parameters influencing the aerodynamic behavior of various liner configurations. As a basis of an analytical study, an extensive experimental database is required. For this purpose, a test rig is set up at the Institute of Thermal Turbomachinery (ITS). Three liner structures (honeycomb, rhombus, and polyhedral structures), two seal fin configurations, and the effect of the adjusted nominal clearances (0.1-1.0 mm) and different pressure conditions are investigated. The experimental results will be presented, discussed, and evaluated by means of established parameters. The focus is on the leakage of the seal, the discharge coefficient, and the equivalent gap width. Additionally, the influence of the geometric shape of the liner structures is discussed. Flow separation and flow direction play the main role. With the results of this paper, optimization guidelines are derived for the design of innovative liner configurations.
Keywords:
Labyrinth Seal - Aerodynamic Flow Field - Innovative Liner Structures - Design Guideline

1. Introduction

With increasing demand for individual mobility, airplanes come into focus. Considering the current climate goals, engineers of new aircraft engines are faced with the major challenge of increasing overall engine efficiency. This would lead to reduced fuel consumption, less pollution, and lower fuel costs. The secondary air system in an aircraft engine offers great potential for optimization. To seal and control the cooling air mass flow between rotating and stationary components, labyrinth seals are applied. The more precisely the cooling air mass flow through the labyrinth seal can be controlled, the less cooling air will be required and the more air will be involved in the primary process of the aircraft engine. The resulting increase in overall efficiency is promising ([1] and [2]).

Due to their non-contact functionality and thermal resistance, labyrinth seals are state-of-the-art in sealing technology of Thermal Turbomachines. Due to thermally induced expansions during operation and transient flight maneuvers as well as the resulting mechanical and thermal loads on the components, a contact, so-called rubbing process, between rotor and stator cannot

be avoided. For an efficient design of the labyrinth seal and, thus, reduced leakage through the seal, the nominal clearance between the components must be as small as possible. This additionally increases the risk of contact. In order to prevent structural damage of vital parts during the rubbing of the components, abradable liners are attached to the stator. These liners have a hollow body structure that leads to a small contact surface and reduces load on the main components and their damage during the rubbing process. Compared to smooth stator surfaces, liner configurations made of hollow body structures increase the cross-sectional area of the sealing gap and, thus, lead to a higher leakage. From an aerodynamic point of view, the liner configuration has to be optimized for minimum leakage without losing its resistance to rubbing. Honeycomb liners made of Hastelloy X sheet metal are state-of-the-art. New production technologies and materials, however, enable the development of innovative liner configurations.
The published studies of sealing performance with regard to innovative liner configurations are of numerical nature exclusively. The aim of this paper is to identify the main geometrical parameters influencing flow and sealing behavior of the various liner configurations. For this purpose, it is necessary to generate an extensive experimental database and to examine it analytically. In this paper, three different liner structures are investigated. As a traditional baseline configuration, honeycomb structures are studied. Additional examinations cover an innovative rhombus structure and a polyhedral cell structure (PCS). To carry out the experiments and to characterize flow behavior of the liner configurations, a planar flow test rig at ITS is used. For a comprehensive overview of the factors influencing the flow behavior, two different seal fin configurations and the effect of the clearance between the seal fin and the liner surface are investigated.
After a brief literature review, the experimental setup is described. To identify the main geometrical parameters, the experimental results will be presented and discussed. The measured data are evaluated using established parameters from literature. Flow characterization focuses on the mass flow rate through the seal, the equivalent gap width, and the discharge coefficient. In a second step, the influence of the geometric shape of the innovative liner structures is discussed based on the investigated parameters. This paper is concluded by a derivation of design guidelines for improved labyrinth seals.

2. Literature Review

The existing literature dealing with the optimization of labyrinth seals can be divided into three main topics: Investigations of the rubbing behavior and the main parameters influencing the load acting on the parts in contact ([3], [4], [5], [6], ...); investigations of the aerodynamic conditions in the labyrinth seal with smooth stators or hollow body structures as liners ([7], [8], [9], [10], [11], [12], [13], [14], ...); and aerodynamic behavior of worn seals ([15], [16], [17], [18], [19], [20], ...). This publication focuses on aerodynamics.
The aim of several studies is to characterize the main variables influencing the aerodynamic flow field in labyrinth seals. In 1975, Stocker et al. investigated flow using different labyrinth seal geometries with a smooth stator in a water tunnel flow visualization test rig. A maximum cavity turbulence was found to result in the lowest leakage mass flows through the seal [21]. In 2001, Willenborg et al. experimentally investigated the influence of the Reynolds number (Re) and pressure ratio on the discharge coefficient. They found that at large Re, the pressure ratio Π is relevant for leakage only [22]. Weinberger et al. carried out a large number of simulations and experiments with different gap widths and honeycomb dimensions ([9], [23], and [12]). Depending on the gap width, honeycomb height, and diameter, different tendencies of flow behavior could be observed. Schramm et al. identified the effective gap width as a geometric influencing parameter s_{eff} for honeycomb liners [24]. With a dimensional analysis and investigations of the influence of pre-swirl and temperature on flow, Denecke et al. contributed to the understanding of the flow

behavior in 2005 ([8] and [25]). They found that the Reynolds number and pressure ratio were among the main parameters influencing the discharge coefficient c_D. Braun et al. focused on the optimization of the seal fin in terms of the leakage behavior of smooth stators ([10], [26], and [11]). With the optimization tool developed by them, the c_D values can be reduced significantly. In 2010, Wroblewski et al. optimized the seal fin geometry of a labyrinth seal with a honeycomb liner [13]. This optimization was repeated by Wroblewski et al. with squeezed honeycomb and rhombus structures that are also used in this publication [14].
The aerodynamic behavior of worn components after rubbing was investigated experimentally and numerically by Stocker et al. [21], Zimmermann et al. [15], Rhode et al. [16] and [17], Denecke et al. [18], and Dogu et al. [20]. For this purpose, rub grooves were manufactured in the stator liners and the seal fin edges were rounded or mushroomed. The increased flow-through cross-sectional area and the radii of the rounded chamfers at the seal fin led to a significant increase in leakage.

3. Experimental Setup

To obtain experimental data, an existing planar flow test rig is modified at ITS. In 2012, Braun et al used this test rig to investigate the flow behavior of a labyrinth seal with a smooth stator. For further information, it is referred to Braun et al. [10]. First, the periphery of the test rig is described, followed by a description of the measuring section as well as the test specimen. Using the infrastructure at ITS, the test rig can be supplied with up to $750 \times 10^{-3}\,\mathrm{kg\,s^{-1}}$ and 9.5 bar clean pressurized air at ambient temperature.

3.1. Test Section

The test section of the experimental setup and the measurement instruments are shown schematically in Figure 1. The mass flow enters the measuring section at the left. A nozzle is mounted directly upstream of the labyrinth to prevent flow separation. The large wall thickness of the housing reduces elongation under pressure. To reduce the wall effect on the sides (tangential, y-direction), the test bench depth is 300 mm. The main part of the measuring section consists of the rotor plates with the integrated seal fins and the stator plates with the glued liner structures. These parts are presented in the next section.

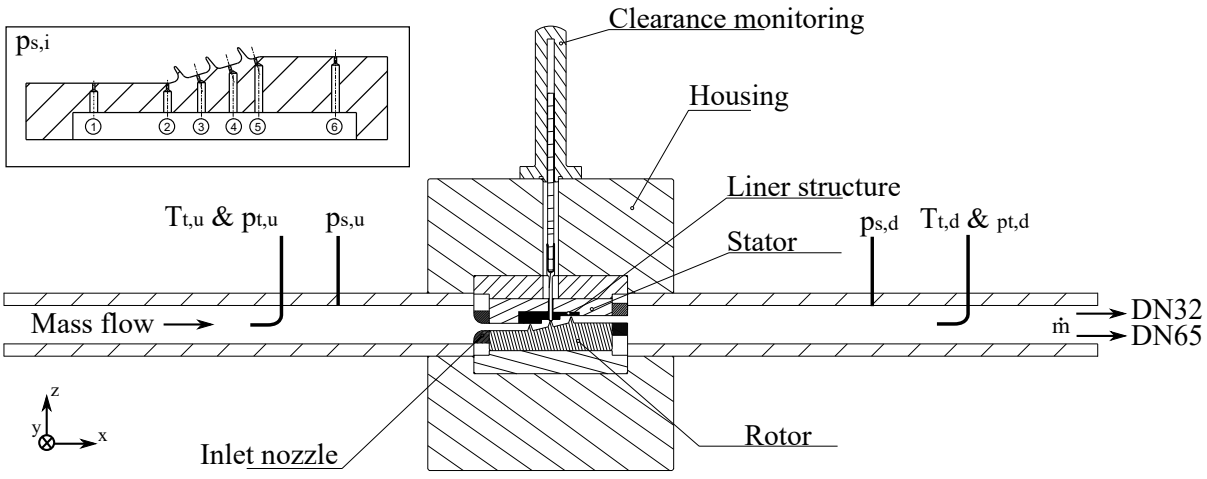

Figure 1: Schematic drawing of the test rig including measurement instruments modified according to Braun et al. [10].

Table 1: Measuring ranges and accuracies of the measuring instruments.

Quantity	Instrument	Range	Accuracy
Static and total p	9116 NetScanner	0 - 6.89 bar	$\pm 3.445 \times 10^{-3}$ bar
p for adjustment ($p_{\mathrm{t,u}}$, $p_{\mathrm{s,d}}$)	WIKA S10	0 - 4 bar	$\pm 10 \times 10^{-3}$ bar
p measuring orifice, absolute	PMP4070	0 - 12 bar	$\pm 4.8 \times 10^{-3}$ bar
p measuring orifice, relative	PMP4170	0 - 200×10^{-3} bar	$\pm 0.08 \times 10^{-3}$ bar
T	Thermocouple type T	-40 - 350 °C	± 0.5 °C
Nominal clearance	Gauge block	—	$\pm 10 \times 10^{-6}$ m
Housing elongation	DTA-15D-S-CA-(03)	—	± 0.35 %

To determine the characteristic flow parameters, pressures, temperatures, distances, and mass flow rates are measured. The accuracies and measuring ranges of the measuring instruments are summarized in Table 1. The measurement accuracies for the calculated quantities will be given in the results section. For their calculation, please refer to Braun et al. [10].

The static and total pressures are measured up- and downstream of the test section. Furthermore, the rotor part is instrumented with static pressure taps. The positions of the taps are marked by 1 through 6 in Figure 1. This enables also the measurement of static pressures directly in the labyrinth chambers. The pressure taps are located at 1/3 (100 mm) and 2/3 (200 mm) of the rig depth in the tangential y-direction. In this way, the pressures are measured redundantly. Total temperature is measured with type T thermocouples at the inlet and outlet of the test section. A mass flow rate dependent switchover between two orifice plates (DN32 and DN65) is used to accurately acquire mass flow rates according to DIN EN ISO 5167. The nominal installed clearance is determined by gauge blocks. In addition, the clearance change due to housing expansion is permanently monitored by means of an inductive distance measurement system. The upstream pressure $p_{\mathrm{t,u}}$ and the back pressure $p_{\mathrm{s,d}}$ are controlled.

3.2. Test Specimen and Test Plan

Two different seal fin geometries and three different liner structures are investigated. Their geometries are shown in Figure 2. Due to confidentiality agreements, the seal fin dimensions cannot be given explicitly.

Three different hollow body liner structures are investigated. The honeycomb liners are used as the reference configuration. Additionally, a polyhedral cell structure and a rhombus structure similar to the geometry studied by Wroblewski et al. in 2018, are analyzed [14]. The geometries are depicted in Figure 3. The important dimensions of the liners are the heights of the structures (H_{HC}, and H_{RH}), the width or length (B_{HC}, B_{PCS}, B_{RH}, and L_{RH}), and the thickness of the structure (t_{HC}, t_{PCS}, and t_{RH}). Due to confidentiality agreements, the liner structure dimensions also cannot be disclosed. It should be noted that the PCS have the smallest structures and that the honeycombs are twice as high, but half as wide as the rhombus. The measured configurations are summarized in Table 2.

Measurements are carried out at ambient temperature. The back pressure is kept at $p_{\mathrm{s,d}} = 2$ bar and the pressure ratio $\Pi = p_{\mathrm{t,u}}/p_{\mathrm{s,d}}$ is gradually increased to 1.02, 1.05, 1.1, 1.15, 1.2, 1.3, 1.5, 1.7, and 2.0. Before each recording, it is ensured that stationary flow conditions prevail. Three radial nominal clearances $s_{\mathrm{nom}} = 0.1\,\mathrm{mm}, 0.5\,\mathrm{mm}, 1.0\,\mathrm{mm}$ are studied.

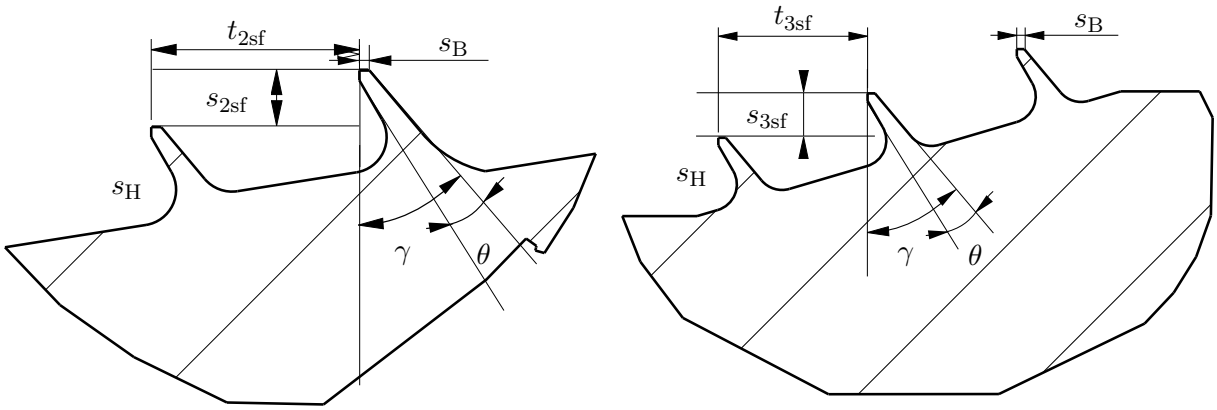

(a) 2 Seal fins (b) 3 Seal fins

Figure 2: Schematic drawings of the seal fin geometries.

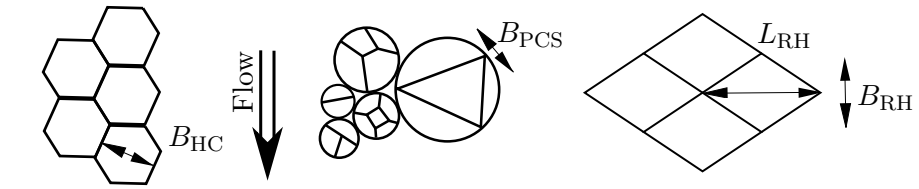

Figure 3: Schematic drawings of the liner geometries.

Table 2: Measured configurations.

Liner	2 seal fins	3 seal fins
Honeycombs	x	x
PCS		x
Rhombus	x	

4. Established Parameters

In this chapter, the established parameters to quantify leakage flow are presented shortly.

Discharge coefficient c_D

The well-known discharge coefficient is used to describe flow losses [7]. c_D is defined as:

$$c_D = \frac{\dot{m}}{\dot{m}_{ideal}}, \tag{1}$$

with

$$\dot{m}_{ideal} = \frac{p_{t,u}A}{\sqrt{T_{t,u}}}\dot{Q}_{ideal} = \frac{p_{t,u}A}{\sqrt{T_{t,u}}}\sqrt{\frac{2\kappa}{R(\kappa-1)}\left[1-\left(\frac{1}{\Pi}\right)^{(\kappa-1)/\kappa}\right]}\left(\frac{1}{\Pi}\right)^{1/\kappa}. \tag{2}$$

To calculate the flow area A, either the adjusted nominal clearance s_{nom} ($c_{\mathrm{D,nom}}$) or the effective clearance s_{eff}

$$s_{\mathrm{eff}} = \sqrt{\left(\frac{B_{\mathrm{liner}} - s_{\mathrm{B}}}{2}\right)^2 + s_{\mathrm{nom}}^2} \tag{3}$$

can be used ($c_{\mathrm{D,eff}}$) [24].

Equivalent gap width
The equivalent gap width s_{eq} can also be taken as a reference parameter [27]. This gap width corresponds to the width of an ideal nozzle passed by the leakage mass flow of the seal. Hence, it is a physical parameter to characterize the influence of the liner structures. s_{eq} is calculated as:

$$s_{\mathrm{eq}} = \frac{\dot{m}\sqrt{T_{\mathrm{t,u}}}}{p_{\mathrm{t,u}}\dot{Q}_{\mathrm{ideal}}B}, \tag{4}$$

with the test rig depth B as relevant dimension.

Reynolds number
To compare the flow phenomena, the Reynolds number Re is calculated as:

$$Re = \frac{\rho v h}{\eta} \approx \frac{2\dot{m}}{\eta B}. \tag{5}$$

5. Results and Discussion

First, general flow in the seal and leakage mass flow through the seal are discussed. The static pressure curve in the labyrinth seal is shown in Figure 4 for the configuration with three seal fins, honeycomb liner structures, different radial clearances, and a pressure ratio Π of 2.0. Additionally, results of a computational fluid dynamics (CFD) study with equivalent boundary conditions are depicted. The Reynolds-averaged Navier-Stokes calculations are performed with an unscaled original test rig geometry. 3D and simplified 2D simulations are carried out. The models are meshed unstructured and have between 690000-19610000 cells. The optimal mesh is found using a mesh independence study according to Ferzinger, 2008 [28]. The simulations are solved pressure-based and with coupled pressure and velocity equations in ANSYSFluent. The turbulence is modelled with the proven k-omega SST turbulence model. Air is calculated as compressible gas with the ideal gas law. The boundary conditions correspond exactly to the conditions prevailing in the experiment: Measured room temperature, back pressure and pressure ratio. The CFD results are not the main topic of this paper and are therefore not explained in more detail. However, they can be used later to explain the flow phenomena, because the pressure curve in the CFD analysis differs from the experimental data by a maximum of 3 %. The positions of the pressure measurement taps are sketched in Figure 1. The pressure curves obtained at the redundant, tangential pressure measuring points and under other pressure conditions are identical. The curves are also similar for other configurations with different liner structures.
The pressure is reduced almost constantly across all chambers. The higher decrease over the last seal fin indicates a higher acceleration. The slightly increased pressure at position 4 with small gap widths (0.1 mm and 0.5 mm) indicates a different vortex formation in the chamber. This is confirmed by the CFD analysis. Also Denecke et al. determined a strong influence of the gap width on the formation of the vortex system in the labyrinth chambers [8]. The lower pressure at 1.0 mm gap width at position 5 directly downstream of the last seal fin compared to position 6 indicates a stronger carry-over effect and a higher flow velocity over the last seal fin. This is also confirmed by the CFD analysis.

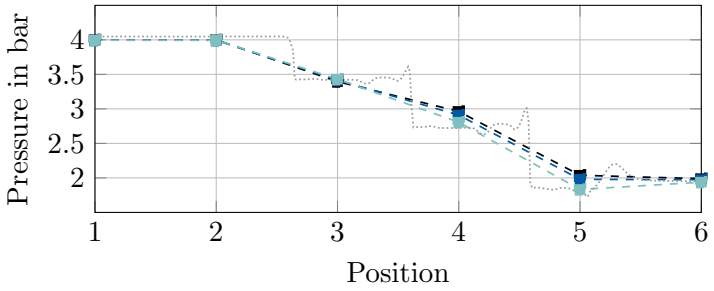

Figure 4: Static pressure at the different measurement positions for the honeycomb liner combined with three seal fins at gap widths of s_{nom} = 0.1 mm (-■-), s_{nom} = 0.5 mm (-■-), and s_{nom} = 1.0 mm (-■-) at a pressure ratio of Π = 2.0. The CFD results for s_{nom} = 1.0 mm are represented by the dotted line ·····.

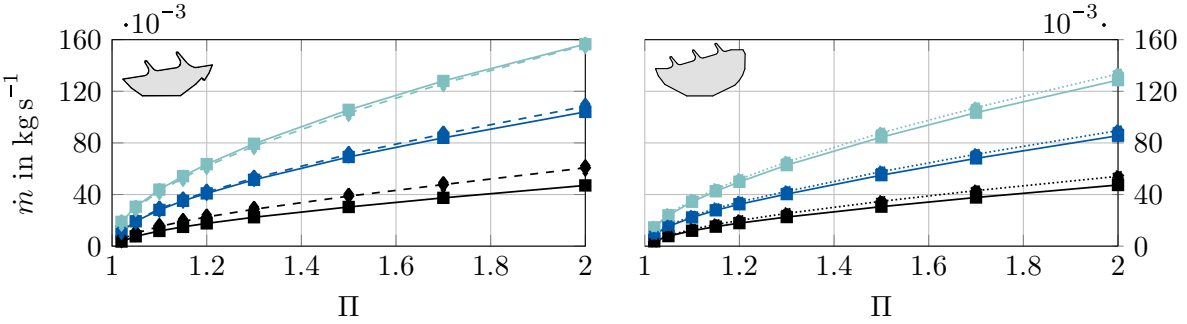

(a) Honeycomb and rhombus with two seal fins (b) Honeycomb and PCS with three seal fins

Figure 5: Mass flow rate $\dot{m}$ as a function of the pressure ratio Π. Lighter colors correspond to larger gap widths, e.g. for the honeycomb liners: s_{nom} = 0.1 mm (—■—), s_{nom} = 0.5 mm (—■—), and s_{nom} = 1.0 mm (—■—). Rhombus liners are marked by (-♦-) and PCS by (···●···).

The leakage mass flow rates $\dot{m}$ of all twelve configurations investigated are plotted against the pressure ratio in Figure 5. While the plots for configurations with two seal fins, honeycomb (—■—), and rhombus structures (-♦-) are shown in Figure 5a, Figure 5b presents the plots for configurations with three seal fins, honeycomb (—■—), and PCS (···●···) structures. Lighter colors indicate larger gap widths. The maximum measuring error of the mass flow rate at a small pressure ratio of Π = 1.02 is ±15.1 %. At Π = 2, the error is ±2.0 %. The mass flow rate through the configurations with two seal fins is higher than that of the configuration with three seal fins. At a gap width of 0.1 mm, this is no longer valid, as the seal will probably choke at the second seal fin. All trends are qualitatively similar: At small pressure ratios, the pressure gradient is larger and at larger pressure ratios, the seal behaves almost like an ideal nozzle. Under the same boundary conditions, the leakage mass flow rate through the seal with innovative liner structures (rhombus structures and PCS) is typically higher than that of the honeycombs. In comparison to the honeycomb liner, the mass flow rate of the rhombus liner is 29.0 % higher at a radial clearance of 0.1 mm. For larger clearances, opposite is true. The maximum mass flow rate through the PCS structures is 14.0 % higher than that of the honeycomb.

5.1. Established Parameters

In order to investigate the flow phenomena in more detail, the experimental results will now be evaluated based on the established parameters.

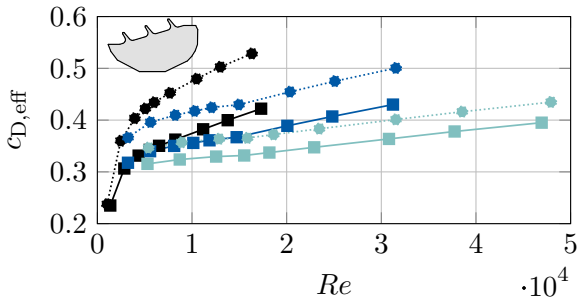

Figure 6: Discharge coefficient $c_{D,eff}$ calculated with s_{eff} as a function of the Reynolds number for the honeycomb (—■—) and PCS (···●···) configurations and three seal fins. Lighter colors indicate higher gap widths (s_{nom} = 0.1, 0.5 and 1.0 mm).

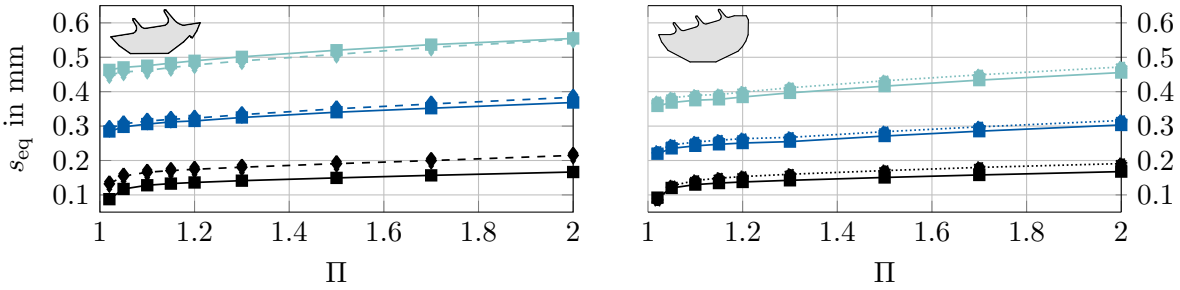

(a) Honeycomb and rhombus with two seal fins

(b) Honeycomb and PCS with three seal fins

Figure 7: Equivalent gap width s_{eq} as a function of the pressure ratio Π for the investigated configurations. Lighter colors correspond to larger gap widths, e.g. for the honeycomb liners: s_{nom} = 0.1 mm (—■—), s_{nom} = 0.5 mm (—■—) and s_{nom} = 1.0 mm (—■—). Rhombus liners are marked with (-♦-) and PCS with (···●···).

In Figure 6 the discharge coefficient $c_{D,eff}$ is depicted as a function of the Reynolds number. The six configurations with three seal fins are shown. Due to the hollow body structures, the flow has much larger passable clearances than s_{nom}. This effect is more pronounced for very small gap widths. For this reason, $c_{D,eff}$ is calculated with the effective gap width s_{eff}. As expected, the discharge coefficient increases with the Reynolds number Re. The effects described by Willenborg et al. [22] and Denecke et al. [18] can also be observed: A strong increase in $c_{D,eff}$ at small Reynolds numbers and a decrease of this gradient due to the more constricted flow. At large Reynolds numbers, $c_{D,eff}$ is expected to be independent of the Reynolds number. However, this effect cannot be determined here, because the measured Reynolds numbers are not large enough.

The equivalent gap width s_{eq} versus the pressure ratio Π is shown in Figure 7 for all investigated configurations. For configurations with two seal fins and the same nominal gap width (Figure 7a), the equivalent gap width is higher than for three seal fins (Figure 7b). At a nominal gap width of 0.1 mm, the equivalent gap width is unexpectedly larger than the nominal gap. This reflects the strong influence of the hollow body structures at small clearances.

5.2. Geometric Liner Shape

The results shown are now discussed in connection with the geometric dimensions of the liner structures.

Comparison: Two seal fins, honeycomb vs. rhombus structure
The height of the rhombus structure is about half the size of the honeycombs. Flow through the seal with honeycomb liners, hence, gets deeper into the structure chambers. The result is a decrease in the leakage mass flow rate for the configurations with honeycombs. According to Weinberger et al., there is a limited saturation due to the flow [12]. The width of the rhombuses in the direction of flow is about 1.35 times larger than the honeycomb width. This leads to a significantly higher effective gap width compared to the nominal gap width of the rhombus structures and explains the significantly higher mass flow (29 %) at a gap width of 0.1 mm compared to honeycombs. When the gap widths increases, this effect is reduced. At 1.0 mm, the leakage mass flow through the rhombus structure is even lower than through the honeycombs, which might be attributed to the sharper edges of the rhombus liner. These lead to a stronger separation of the flow at the liner and, as a result, to a smaller vena contracta.

Comparison: Three seal fins, honeycomb vs. PCS
The cells of the PCS are smaller than a honeycomb cell. Nevertheless, their sealing efficiency is lower. Supporting CFD studies were also made. They revealed that the detachment at the cells is lower and flow is less swirled in the cells due to their spherical structures. Furthermore, the height of the cells is significantly lower, which also leads to a less turbulent flow through the seal. In addition, the cells of the PCS liner are only connected at one point. This results in small gaps in the structure. The airflow passing these gaps further increases the leakage mass flow.

5.3. Design Guidelines
From the presented experimental results and geometric influences identified, some guidelines can be derived for the design of the liner structures:

- The width of the hollow body cells in the direction of flow should not be too large. If the nominal gap width is small, the effective flow area will increase considerably.
- The structures should lead to the highest possible cavity turbulence over the labyrinth seal. This is ensured by a good intrusion of flow into the cell cavities and a high turbulence of the flow there. An inclination of the seal fin can support this. Round structures lead to a less turbulent flow. In addition, the height of the liners should be high enough to guide a sufficient amount of flow into the chambers, thus dissipating energy and reducing the carry-over effect.
- The edges of the seal fin and the liner structure cells should be as sharp as possible. The separation leads to a very small vena contracta and, hence, to a strong reduction of the leakage mass flow rate.

6. Conclusion
This paper presented experiments for the investigation of the aerodynamic flow behavior of labyrinth seals. Three different liner structures, two seal fin variations, three nominal gap widths, and nine pressure conditions yielded 108 data points. These data were used to determine the influence of the geometric dimensions of the liner structures on the sealing behavior. It was found that the innovative liners (rhombus structures and polyhedral cell structures) often lead to a higher leakage mass flow compared to honeycomb liner structures. The reasons identified were large cell dimensions, round cell bodies, and gaps in the liners. The sharp edges of the rhombus structures compensated the increase in mass flow rate by the coarse cells. Further measurements and simulations with specific parameter variations are planned. Rubbing behavior is not considered yet.

Nomenclature

A	mm^2	Area
B	mm	Width
c_D	—	Discharge coefficient
H	mm	Hight
h	mm	Hydraulic diameter
L	mm	Length
$\dot{m}$	kg/s	Mass flow rate
p	bar	Pressure
$\dot{Q}$	$s\sqrt{K}/m$	Mass flow rate
R	J/(Kg K)	Specific gas constant
s	mm	Clearance
s_B	mm	Seal fin thickness
s_H	mm	Seal fin hight
T	K	Temperature
t	mm	Thickness
t_{2sf}, t_{3sf}	mm	Distance between seal fins
v	m/s	Velocity
γ, Θ	$^\circ$	Angels of seal fins
Π	—	Pressure ratio
κ	—	Isotropic exponent
ρ	kg/m^2	Density
η	kg/(m s)	Dynamic viscosity

Subscripts

d	Downstream
eff	Effective
HC	Honeycombs
ideal	Ideal
liner	Liner structure
nom	Nominal
PCS	Polyhedron cell structures
RH	Rhombus structure
s	Static
t	Total
u	Upstream

Acknowledgments
The authors gratefully acknowledge the support of this project by Rolls-Royce Deutschland Ltd & CO KG and the Federal Ministry for Economic Affairs and Energy (BMWi) within the framework of the AGTurbo project EcoFLEX 3.1.2.

References

[1] Bräunling, W. J. G., 2015. *Flugzeugtriebwerke: Grundlagen, Aero-Thermodynamik, ideale und reale Kreisprozesse, Thermische Turbomaschinen, Komponenten, Emissionen und Systeme*, 4. ed. Springer Vieweg, Berlin.

[2] Rossmann, A., 2001. *Die Sicherheit von Turbo-Flugtriebwerken. Band 2. Reibverschleiss, Anstreifen und Spalthaltung, Labyrinthe, Bürstendichtungen, Containment, Feuer und Expolsionen.*, 1. ed. Turbo Consult, Karlsfeld.

[3] Pychynski, T., Höfler, C., and Bauer, H.-J., 2016. "Experimental study on the friction contact between a labyrinth seal fin and a honeycomb stator". *Journal of Engineering for Gas Turbines and Power,* ***138***(6).

[4] Munz, O., Schwitzke, C., Bauer, H.-J., Welzenbach, S., Fischer, T., and Ulan kyzy, S., 2018. "Modelling the rubbing process in labyrinth seals". In Proceedings of GPPS Forum 18, Zurich, CH, January 10-12, 2018, no. GPPS-2018-0038/ 1-9.

[5] Munz, O., Pychynski, T., Schwitzke, C., and Bauer, H.-J., 2018. "Continued experimental study on the friction contact between a labyrinth seal fin and a honeycomb stator: Slanted position". *Aerospace,* ***5***(3), p. 82.

[6] Fischer, T., Welzenbach, S., Meier, F., Werner, E., Ulan kyzy, S., and Munz, O., 2018. "Modeling the rubbing contact in honeycomb seals". *Continuum Mechanics and Thermodynamics,* ***30***(2), pp. 381–395.

[7] Wittig, S. L. K., Dörr, L., and Kim, S., 1983. "Scaling effects on leakage losses in labyrinth seals". *Journal of Engineering for Power,* ***105***(2), pp. 305–309.

[8] Denecke, J., Dullenkopf, K., Wittig, S., and Bauer, H.-J., June 6–9, 2005. "Experimental investigation of the total temperature increase and swirl development in rotating labyrinth seals". In ASME Turbo Expo 2005: Power for Land, Sea, and Air, pp. 1161–1171.

[9] Weinberger, T., Dullenkopf, K., and Bauer, H. J., 2011. "Influence of honeycomb facings on the temperature distribution of labyrinth seals". *Turbo Expo: Power for Land, Sea, and Air, Volume 4: Heat Transfer, Parts A and B*, pp. 921–930.

[10] Braun, E., Dullenkopf, K., and Bauer, H.-J., 2012. "Optimization of labyrinth seal performance combining experimental, numerical and data mining methods". In ASME Turbo Expo 2012: Turbine Technical Conference and Exposition, p. 1847.

[11] Braun, E., 2016. "Ein Beitrag zur Formoptimierung von Labyrinthdichtungen". PhD thesis, Karlsruhe, Institut für Thermische Strömungsmaschinen.

[12] Weinberger, T., 2014. "Einfluss geometrischer Labyrinth- und Honigwabenparameter auf das Durchfluss- und Wärmeübergangsverhalten von Labyrinthdichtungen: Experiment, Numerik und Data Mining". PhD thesis, Karlsruhe, Institut für Thermische Strömungsmaschinen.

[13] Wroblewski, W., Dykas, S., B. K., and Rulik, S., 2010. "Optimization of tip seal with honeycomb land in lp counter rotating gas turbine engine". *Task Quarterly,* ***14***, pp. 189–207.

[14] Wroblewski, W., Frkaczek, D., and Marugi, K., 2018. "Leakage reduction by optimisation of the straight–through labyrinth seal with a honeycomb and alternative land configurations". *International Journal of Heat and Mass Transfer,* ***126***, pp. 725–739.

[15] Zimmerman, H., Kammerer, A., and Wolff, K. H., 1994. "Performance of worn labyrinth seals". In Volume 1: Turbomachinery, ASME.

[16] Rhode, D. L., and Allen, B. F., 1998. "Visualization and measurements of rub-groove leakage effects on straight-through labyrinth seals". Vol. Volume 4: Heat Transfer; Electric Power; Industrial and Cogeneration of *Turbo Expo: Power for Land, Sea, and Air*.

[17] Rhode, D. L., and Allen, B. F., 2000. "Measurement and visualization of leakage effects of rounded teeth tips and rub-grooves on stepped labyrinths". *Journal of Engineering for Gas Turbines and Power,* ***123***(3), pp. 604–611.

[18] Denecke, J., Schramm, V., Kim, S., and Wittig, S., 2003. "Influence of rub-grooves on labyrinth seal leakage". *Journal of Turbomachinery,* ***125***(2), p. 387.

[19] Dogu, Y., Sertçakan, M. C., Gezer, K., Kocagül, M., Arican, E., and Ozmusul, M. S., 2017. "Labyrinth seal leakage degradation due to various types of wear". *Journal of Engineering for Gas Turbines and Power,* ***139***(6).

[20] Dogu, Y., Sertçakan, M. C., Gezer, K., Kocagül, M., Arican, E., and Ozmusul, M. S., 2017. "Leakage degradation of straight labyrinth seal due to wear of round tooth tip and acute trapezoidal rub-groove". *Journal of Engineering for Gas Turbines and Power,* ***139***(7).

[21] Stocker, H. L., 1975. "Advanced labyrinth seal design performance for high pressure ratio gas turbines". *ASME 1975 Winter Annual Meeting: GT Papers, Turbo Expo: Power for Land, Sea, and Air*.

[22] Willenborg, K., Kim, S., and Wittig, S., 2001. "Effects of Reynolds number and pressure ratio on leakage loss and heat transfer in a stepped labyrinth seal". *Journal of turbomachinery 123 (2001) H. 4 und in: Proceedings of the 46th ASME Turbo Expo, New Orleans, La. 2001.*

[23] Weinberger, T., Dullenkopf, K., and Bauer, H. J., 2010. "Numerical approach to study the influence of honeycomb facings on the temperature distribution of labyrinth seals". *ISROMAC 13, 13th International Symposium on Transport Phenomena and Dynamics of Rotating Machinery, Honolulu*, pp. 439–447.
[24] Schramm, V., Willenborg, K., Kim, S., and Wittig, S., May 8-11, 2000. "Influence of a honeycomb facing on the flow through a stepped labyrinth seal". In ASME Turbo Expo 2000: Power for Land, Sea, and Air.
[25] Denecke, J., Färber, J., Dullenkopf, K., and Bauer, H.-J., June 6–9, 2005. "Dimensional analysis and scaling of rotating seals". In ASME Turbo Expo 2005: Power for Land, Sea, and Air, pp. 1149–1160.
[26] Braun, E., Pychynski, T., and Bauer, H.-J., 2014. "An opensource framework for multi-objective flow optimization as applied to labyrinth seals". In 15th International Symposium on Transport Phenomena and Dynamics of Rotating Machinery, ISROMAC-15 Honolulu, Hawaii; February 24 - 28, 2014, ISROMAC.
[27] Jahn, I. H. J., Owen, A. K., Franceschini, G., and Gillespie, D., 2008. "Experimental characterisation of the stiffness and leakage of a prototype leaf seal for turbine applications". Vol. Volume 4: Heat Transfer, Parts A and B of *Turbo Expo: Power for Land, Sea, and Air*, pp. 1657–1666.
[28] Ferziger, J. H., 2008. *Numerische Strmungsmechanik*. SpringerLink. Berlin, Heidelberg.